Characterization of a Class of Waveguide Discontinuities Using a Modified TE^x_{mn} Mode Approach

JENS BORNEMANN, SENIOR MEMBER, IEEE, AND RUEDIGER VAHLDIECK, SENIOR MEMBER, IEEE

Abstract —**This paper presents a modified TE^x_{mn} wave approach which is used in conjunction with the mode matching method for the field-theory modeling of a class of waveguide discontinuities. In particular, for characterizing waveguide discontinuities in which resonant effects occur, this method resolves conflicting results which have been observed using the conventional TE^x_{mn} mode matching technique, commonly known from the literature, and the generalized analysis based on a linear superposition of TE^z_{mn} and TM^z_{mn} modes. It is found that results from the modified TE^x_{mn} mode approach are consistent with the generalized analysis and agree well with measurements on iris filters and corrugated waveguide polarizers. In comparison with the generalized TE–TM mode analysis, the modified TE^x_{mn} mode procedure consumes less memory and CPU time and provides improved convergence behavior without sacrificing design accuracy.**

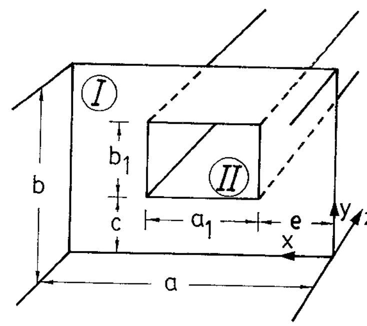

Fig. 1. Double-step discontinuity in rectangular waveguide.

I. Introduction

Modern microwave and millimeter-wave computer-aided design packages are based on numerically efficient yet accurate computation techniques for the field-theory modeling of circuit discontinuities. In particular, computer-aided design of waveguide components at millimeter wavelengths requires accurate computation of circuit S parameters to avoid or minimize cut-and-try manufacturing cycles.

In this paper, we will investigate different approaches for characterizing single- or double-plane discontinuities which are integral design elements for a wide range of waveguide components such as transformers [1], [3], [4], iris and corrugated waveguide filters [1]–[3], [5], [6], evanescent-mode band-pass filters [7]–[10], horn antennas [11], [12], and polarizers [11]–[16].

Numerical characterization of the type of waveguide junction discontinuities shown in Fig. 1 is usually carried out by a generalized analysis utilizing a linear superposition of TE_{mn}–TM_{mn} modes. Based on the assumption that an incident TE_{10} wave would excite TE_{mn} and TM_{mn} waves, two vector potential functions are necessary to describe the four field components (E_x, E_y, H_x, H_y) to be matched at $z = 0$ [3]–[5]. However, the double-plane step discontinuity can be viewed as a combination of two single-plane steps in which only the E-plane discontinuity introduces an E_x component through, e.g., the $TE_{1,2}$ and the $TM_{1,2}$ modes. On the other hand, field computations using the TE_{mn}–TM_{mn} approach have indicated that this E_x component is fairly small, and by neglecting this component no significant error is introduced. This assumption has already been used in [18] and [19] to characterize E-plane discontinuities for diplexer applications. In these papers, a TE^x_{mn} approach has been utilized which automatically excludes the existence of an E_x component. The advantage of this approach over the TE_{mn}–TM_{mn} approach is that in the latter case many higher order terms in the continuity equations are necessary to approximate a small or even zero E_x-field component. In the TE^x_{mn} approach, the E_x field is assumed to be zero, allowing much faster converging results. In other words, the number of modes required to model the field at the discontinuity is reduced to N_{TE}, compared with $M_{TE} + P_{TM}$ for the TE–TM mode case [17] (in general, $M > N \approx P$). This significantly speeds up the calculations and, at the same time, reduces the storage requirements.

This procedure has been successfully applied in some special cases [8], [17]–[19]. In cases, however, where resonant effects occur in the discontinuity plane, conflicting results with the TE_{mn}–TM_{mn} mode approach have been observed. This discrepancy is due to the fact that in the TE^x_{mn} mode approach, the resulting equation system contains two unknowns but, rigorously, requires three field components (E_y, H_x, H_y) to be matched. In many applications, neglecting the H_y component in the matching conditions does not lead to wrong results. In other cases, however, it does. Therefore, this paper focuses on a

Manuscript received March 27, 1990; revised July 31, 1990.
The authors are with the Department of Electrical and Computer Engineering, University of Victoria, P.O. Box 1700, Victoria, B.C., Canada V8W 2Y2.
IEEE Log Number 9038996.

0018-9480/90/1200-1816$01.00

modified TE^x_{mn} mode approach and its comparison with results obtained by the conventional TE-to-x and the generalized TE–TM mode procedure. In particular, the three different analysis methods are:

Method 1: The conventional TE^x_{mn} mode method, where only E_y and H_x are matched.
Method 2: The modified TE^x_{mn} mode procedure matching E_y and H_x or H_y alternatively.
Method 3: The generalized TE–TM mode analysis matching the field components E_x, E_y, H_x, H_y.

The excellent agreement between the modified TE^x_{mn} routine (method 2), the TE–TM mode analysis (method 3), and measurements is demonstrated for the examples of resonant iris filters and corrugated waveguide polarizers.

II. Theory

In this section, only the basic steps of the modified TE^x_{mn} mode formulation are presented. For details on the generalized TE_{mn}–TM_{mn} mode field description and the corresponding modal scattering matrix calculation, the reader is referred to [20].

In the case of the TE^x_{mn} mode representation, the transverse field components in region $i = \mathrm{I, II}$ (c.f. Fig. 1),

$$E^i_y = \frac{\partial}{\partial z} A^i_{hx}$$
$$H^i_x = \frac{j}{\omega\mu_0}\left[k_0^2 + \frac{\partial^2}{\partial x^2}\right] A^i_{hx}$$
$$H^i_y = \frac{j}{\omega\mu_0}\frac{\partial^2}{\partial x \partial y} A^i_{hx} \tag{1}$$

are derived from the x component of a vector potential

$$A^i_{hx} = 2\sum_{q=1}^{\infty}\sqrt{\frac{\omega\mu_0/k^i_{zq}}{F^i_\square\left[k_0^2-\left(k^i_{xm}\right)^2\right]}}\,T^i_{mn}(x,y) \cdot\left(V^i_q e^{-jk^i_{zq}z} - R^i_q e^{+jk^i_{zq}z}\right) \tag{2}$$

where V^i_q and R^i_q are the wave amplitudes traveling in the positive and negative z direction, respectively, and $F^i_\square$ equals $a\cdot b$ (region I) or $a_1\cdot b_1$ (region II). The index q is related to combinations (m,n) of the waveguide cross-section functions

$$T^{\mathrm{I}}_{mn}(x,y) = \sin\left\{(2m-1)\frac{\pi}{a}x\right\}\cos\left\{\frac{2n\pi}{b}y\right\}\Big/\sqrt{1+\delta_{on}}$$
$$T^{\mathrm{II}}_{mn}(x,y) = \sin\left\{(2m-1)\frac{\pi}{a_1}(x-e)\right\} \cdot\cos\left\{\frac{2n\pi}{b_1}(y-c)\right\}\Big/\sqrt{1+\delta_{on}} \tag{3}$$

(δ_{on} = Kronecker delta)

by rearranging them with respect to increasing cutoff frequencies, e.g.,

$$k^i_{zq} = k^i_{zmn} = \sqrt{k_0^2 - \left(k^i_{xm}\right)^2 - \left(k^i_{yn}\right)^2}. \tag{4}$$

The square root function in (2) is determined by a power normalization for each mode:

$$P^i_q = \begin{cases} 1W & \text{propagating mode} \quad \left[k_0^2 > \left(k^i_{xm}\right)^2 + \left(k^i_{yn}\right)^2\right] \\ -jW & \text{evanescent mode} \quad \left[k_0^2 > \left(k^i_{xm}\right)^2\right] \\ +jW & \text{evanescent mode} \quad \left[k_0^2 < \left(k^i_{xm}\right)^2\right] \end{cases} \tag{5}$$

which shows that the TE^x_{mn} formulation presented here satisfies the same conditions in terms of real and reactive power as required for the TE_{mn}–TM_{mn} mode description (c.f. [20]).

Matching the field components of (1) at the common interface of regions I and II and truncating the infinite sums in (2) yields three matrix equations:

$$E_y: \quad \boldsymbol{V}^{\mathrm{I}} + \boldsymbol{R}^{\mathrm{I}} = \boldsymbol{L}_E(\boldsymbol{V}^{\mathrm{II}} + \boldsymbol{R}^{\mathrm{II}}) \tag{6}$$
$$H_x: \quad \boldsymbol{L}_{Hx}(\boldsymbol{V}^{\mathrm{I}} - \boldsymbol{R}^{\mathrm{I}}) = \boldsymbol{V}^{\mathrm{II}} - \boldsymbol{R}^{\mathrm{II}} \tag{7}$$
$$H_y: \quad \boldsymbol{L}_{Hy}(\boldsymbol{V}^{\mathrm{I}} - \boldsymbol{R}^{\mathrm{I}}) = \boldsymbol{V}^{\mathrm{II}} - \boldsymbol{R}^{\mathrm{II}} \tag{8}$$

with the matrix elements given by

$$(\boldsymbol{L}_E)_{pq} = \frac{4}{\sqrt{F^{\mathrm{I}}_\square F^{\mathrm{II}}_\square}}\sqrt{\frac{k^{\mathrm{II}}_{zq}\left[k_0^2-\left(k^{\mathrm{I}}_{xp}\right)^2\right]}{k^{\mathrm{I}}_{zp}\left[k_0^2-\left(k^{\mathrm{II}}_{xq}\right)^2\right]}}\int_{F^{\mathrm{II}}_\square} T^{\mathrm{I}}_p T^{\mathrm{II}}_q \, dF \tag{9}$$

$$(\boldsymbol{L}_{Hx}) = (\boldsymbol{L}_E)^T \qquad T = \text{transposed} \tag{10}$$

$$(\boldsymbol{L}_{Hy})_{qp} = \frac{4}{\sqrt{F^{\mathrm{I}}_\square F^{\mathrm{II}}_\square}}\sqrt{\frac{k^{\mathrm{II}}_{zq}\left[k_0^2-\left(k^{\mathrm{II}}_{xq}\right)^2\right]}{k^{\mathrm{I}}_{zp}\left[k_0^2-\left(k^{\mathrm{I}}_{xp}\right)^2\right]}}\frac{1}{\left(k^{\mathrm{II}}_{xq}\right)^2\left(k^{\mathrm{I}}_{xp}\right)^2} \cdot\int_{F^{\mathrm{II}}_\square}\frac{\partial}{\partial x\partial y}T^{\mathrm{I}}_p\frac{\partial}{\partial x\partial y}T^{\mathrm{II}}_q \, dF. \tag{11}$$

To calculate the modal scattering matrix of the double-step discontinuity,

$$\begin{bmatrix}\boldsymbol{R}^{\mathrm{I}}\\ \boldsymbol{V}^{\mathrm{II}}\end{bmatrix} = (\boldsymbol{S})\begin{bmatrix}\boldsymbol{V}^{\mathrm{I}}\\ \boldsymbol{R}^{\mathrm{II}}\end{bmatrix} \tag{12}$$

only two equations of the set (6)–(8) are needed to separate the two unknowns $\boldsymbol{R}^{\mathrm{I}}$ and $\boldsymbol{V}^{\mathrm{II}}$. Matching E_y and H_x and ignoring H_y leads to excellent results in some special cases, e.g. [18] and [19], but leads to wrong results for resonating double-step discontinuities. On the other hand, merely considering E_y and H_y for the matching conditions or, alternatively, H_x and H_y lacks information in the presence of TE^x_{m0} modes.

Therefore, the following modified TE^x_{mn} procedure is proposed here. First, E_y is matched using (6) and (9), and matrices $\boldsymbol{L}_{Hx}$ and $\boldsymbol{L}_{Hy}$ are calculated according to (10) and (11), respectively. A new matrix ($\boldsymbol{L}_H$) is then formed by copying elements from either $\boldsymbol{L}_{Hx}$ or $\boldsymbol{L}_{Hy}$ into $\boldsymbol{L}_H$ where

$$\begin{aligned}
(\boldsymbol{L}_H)_{qp} &= (\boldsymbol{L}_{Hx})_{qp} && \text{if mode } q \text{ or mode } p \text{ is a } \mathrm{TE}^x_{m0} \text{ type.}\\
(\boldsymbol{L}_H)_{qp} &= (\boldsymbol{L}_{Hy})_{qp} && \text{if neither mode } q \text{ nor mode } p \text{ is a } \mathrm{TE}^x_{m0} \text{ type.}
\end{aligned} \tag{13}$$

Consequently, $\boldsymbol{L}_H$ contains data which are derived from matching conditions of either H_x or H_y. Hence this procedure merges (7) and (8) into one equation and allows the resulting matrix system (6)–(8) to be solved for its unknowns $\boldsymbol{R}^{\mathrm{I}}$ and $\boldsymbol{V}^{\mathrm{II}}$.

The modal scattering matrix of the double-step discontinuity

$$\begin{aligned}
\boldsymbol{S}_{11} &= [\boldsymbol{L}_E\boldsymbol{L}_H + \boldsymbol{U}]^{-1}[\boldsymbol{L}_E\boldsymbol{L}_H - \boldsymbol{U}]\\
\boldsymbol{S}_{12} &= 2[\boldsymbol{L}_E\boldsymbol{L}_H + \boldsymbol{U}]^{-1}\boldsymbol{L}_E\\
\boldsymbol{S}_{21} &= \boldsymbol{L}_H[\boldsymbol{U} - \boldsymbol{S}_{11}]\\
\boldsymbol{S}_{22} &= \boldsymbol{U} - \boldsymbol{L}_H\boldsymbol{S}_{12}, \qquad \boldsymbol{U} = \text{unit matrix}
\end{aligned} \tag{14}$$

calculated under the condition (13) shows excellent agreement with measured data. Compared with the TE–TM analysis, this new procedure considerably reduces the matrix sizes to be processed by the computer. Moreover, the fact that a smaller number of modes interact between discontinuities than in the discontinuity plane itself can be easily implemented in this approach. By these measures, the processing time of the algorithm can be made up to five times faster. (For further derivations leading to the modal scattering matrix of cascaded discontinuities, the reader is referred to [20] and [21].)

III. Results

Waveguide iris filters can operate in two different modes. In the first category, half-wave resonators are connected by irises which act as coupling elements only. The transmission behavior of a single iris is shown in Fig. 2. The three methods investigated yield identical results within the plotting accuracy. Therefore, excellent agreement is usually obtained by all three methods when compared with measured data of an iris-coupled half-wave resonator filter. This is demonstrated in Fig. 3 using measurements carried out in [5]. However, the TE^x_{mn} procedures (methods 1 and 2) require only 30% of the CPU time needed in the generalized TE–TM analysis (method 3).

In the second category, the iris filter utilizes the resonances of the irises itself rather than waveguide resonators. In this mode, the irises are required to operate above cutoff, which occurs at 37.5 GHz in the example of Fig. 4. Exactly at this frequency, the first method reveals some instabilities due to the lack of H_y field matching, whereas the other two methods are in good agreement in modeling the resonance effect of the iris. Fig. 5 shows a comparison with measured data on this type of iris filter

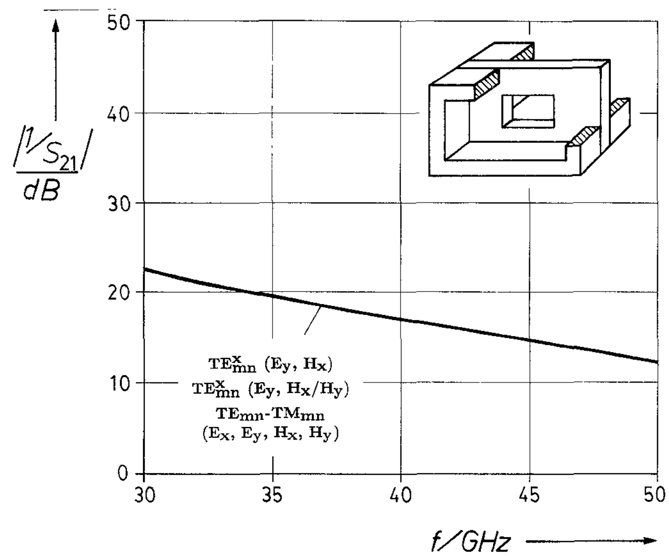

Fig. 2. Insertion loss of a nonresonant iris in rectangular waveguide ($a = 2b = 7.112$ mm, $a_1 = b_1 = 2$ mm, iris thickness = 0.5 mm). Results of all methods investigated within plotting accuracy.

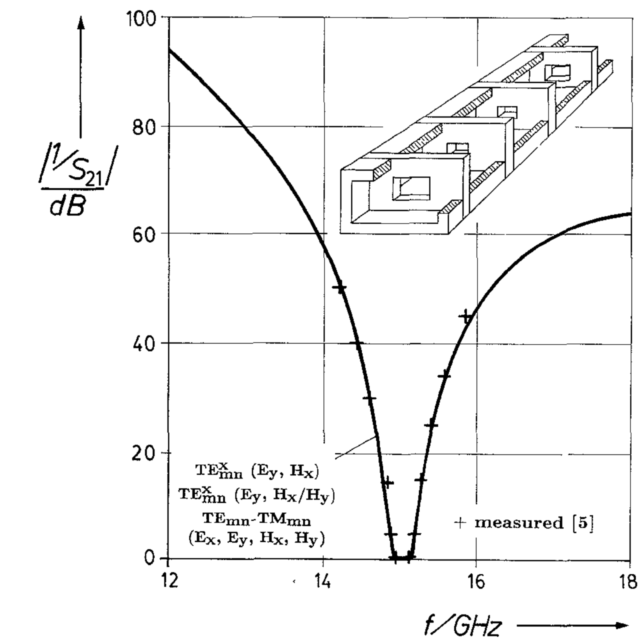

Fig. 3. Insertion loss of three-resonator iris-coupled *Ku*-band waveguide filter according to Tucholke [5] (—— theoretical results obtained by all three methods; + + measured [5]).

presented by Chen [2]. As expected from the results of Fig. 4, the conventional TE^x_{mn} analysis matching E_y and H_x (method 1) leads to incorrect results for the filter insertion (and return) loss, while, surprisingly enough, the bandwidth and the stopband attenuation are almost identical to the other two methods. Methods 2 and 3 show identical results, which closely agree with measurements. In terms of the CPU time required, the ratio of 1:5 in favor of the new TE^x_{mn} analysis (method 2) clearly demonstrates its advantage over the generalized TE–TM procedure.

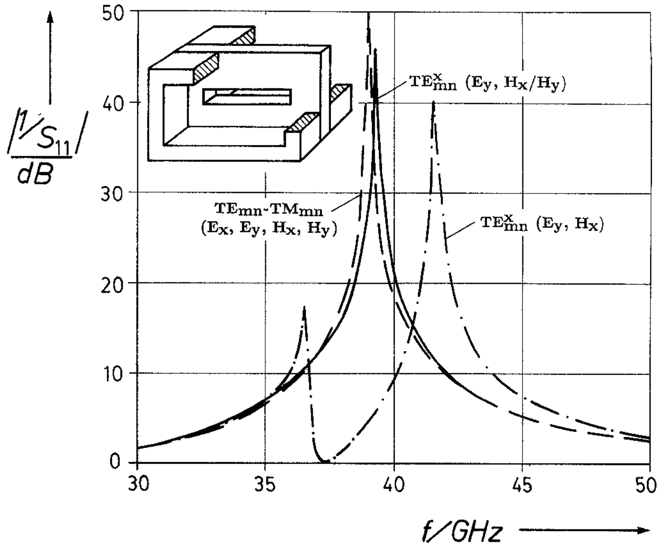

Fig. 4. Return loss of resonant iris in rectangular waveguide ($a = 2b = 7.112$ mm, $a_1 = 4$ mm, $b_1 = 1$ mm, iris thickness = 0.5 mm). Methods of analysis using —·—·—TE^x_{mn} modes matching E_y, H_x (method 1); —— TE^x_{mn} modes matching $E_y, H_x/H_y$ (method 2); ----TE–TM modes matching E_x, E_y, H_x, H_y (method 3).

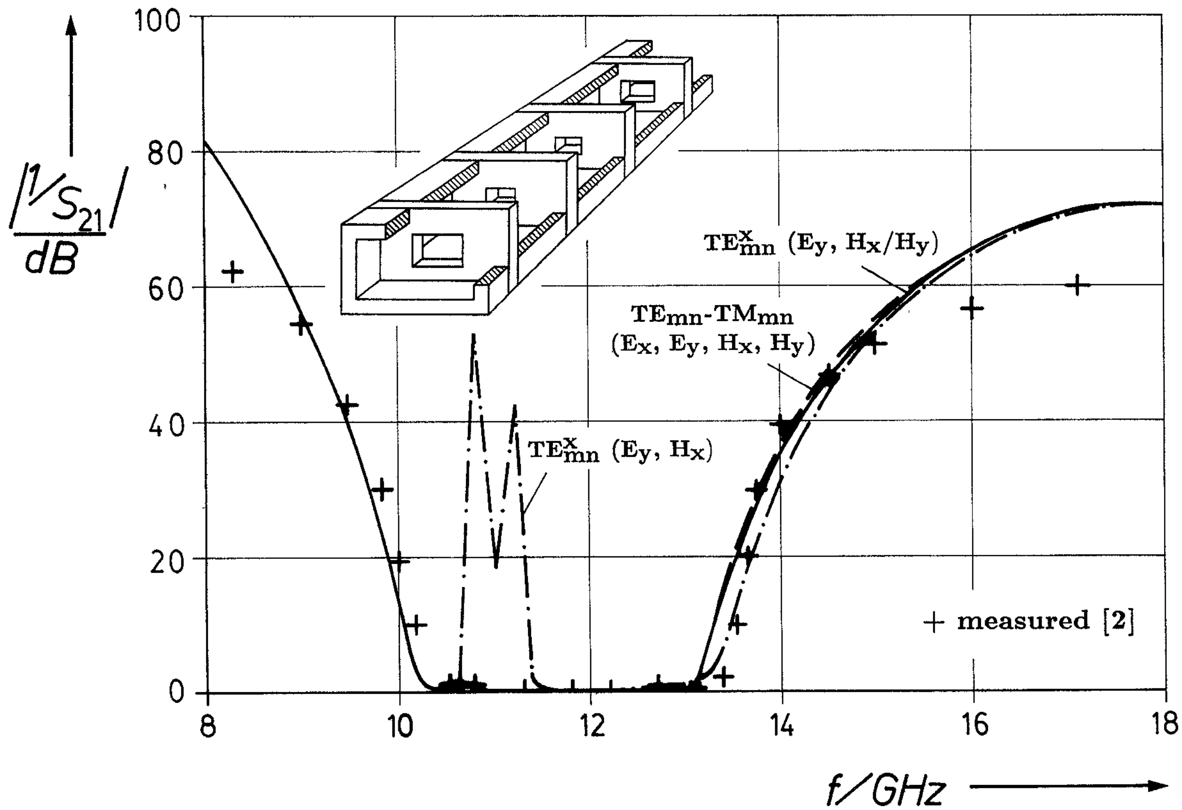

Fig. 5. Comparison between theories and measurements for the example of an X-band seven resonant-iris waveguide filter according to Chen [2] (+ + measured [2]; sets of modes as in Fig. 4).

Finally, the new approach is tested against measured data of E-plane corrugated waveguide square polarizers. Although the discontinuities involved are not double-plane steps in general, both discontinuity planes are involved when the transmission phase difference between a TE_{01} and the orthogonal TE_{10} mode excitation is calculated. Since the structure consists of 22 capacitive (TE_{10}) or inductive (TE_{01}) irises, phase relations are very critical. Fig. 6(a) shows a comparison with phase difference measurements presented by Dewey [11]. The agreement is extremely close, thereby verifying the phase accuracy of this new method. Moreover, the calculated input return

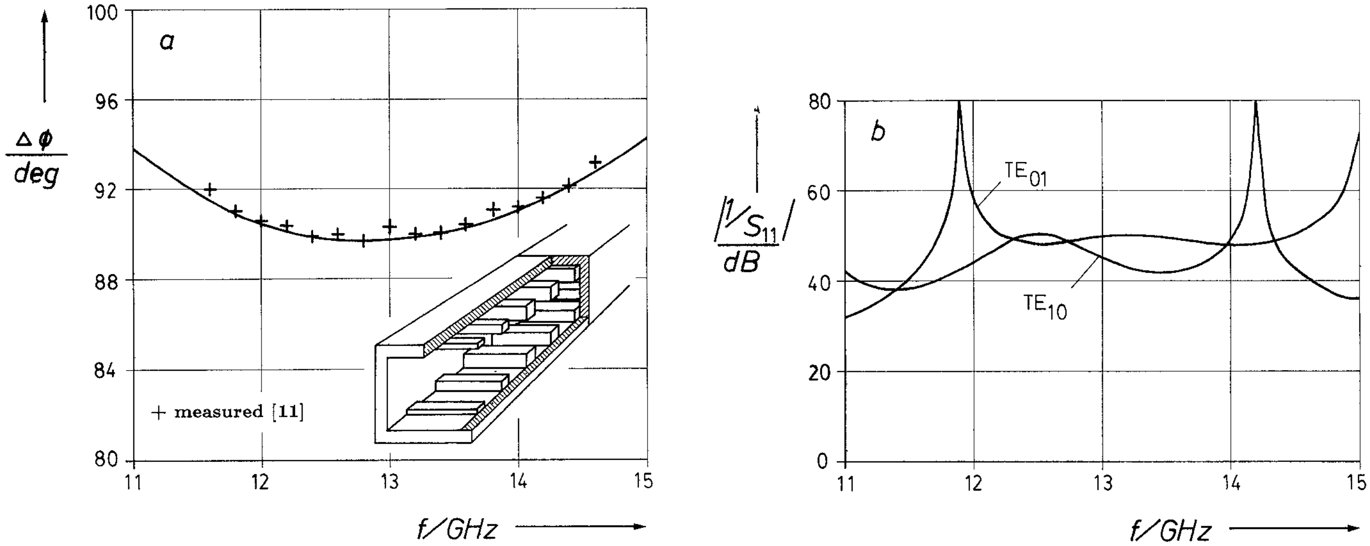

(a) (b)

Fig. 6. E-plane corrugated waveguide polarizer according to Dewey [11] (—— TE^{x}_{mn} mode theory with $E_y, H_x/H_y$ matching (method 2)). (a) Differential phase shift $\Delta\phi = \phi(TE_{01}) - \phi(TE_{10})$ (+ +measured [11]). (b) Calculated input return loss for TE_{01} and TE_{10} mode excitation.

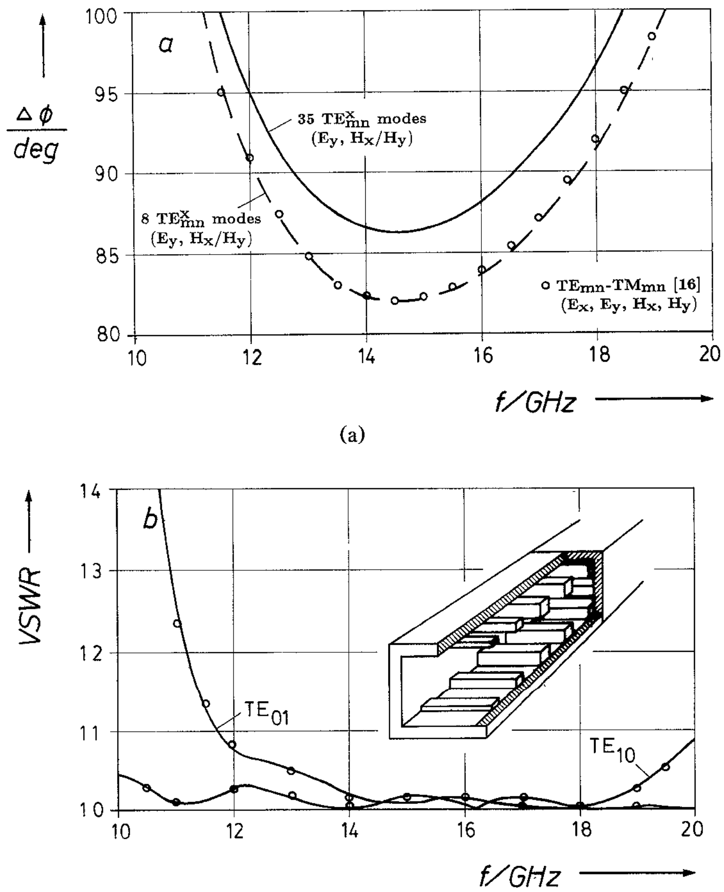

(b)

Fig. 7. Polarizer design with linearly tapered corrugation according to [16]; methods of analysis using 8 (– – – –) and 35 (————) TE^{x}_{mn} modes matching $E_y, H_x/H_y$ (method 2); ∘∘∘ TE_{mn}–TM_{mn} modes matching E_x, E_y, H_x, H_y (method 3) [16]. (a) Differential phase shift. (b) VSWR.

loss values of TE_{10} and TE_{01} mode excitation (Fig. 6(b)) are within the measured margins specified in [11]: return loss (TE_{10}) better than 36.5 and 40 dB for 12–12.5 GHz and 14–14.5 GHz, respectively; return loss (TE_{01}) better than 34 and 40 dB in the same frequency ranges. Nearly identical results are obtained with a TE–TM mode analysis, as presented in [16].

Fig. 7(a) shows the differential phase shift of a linearly tapered corrugated polarizer which has been designed using the TE–TM mode analysis [16]. Although calculations with eight TE^x_{mn} modes are in good agreement with the performance given in [16], computations using 35 modes as a result of a convergence analysis reveal deviations of more than 4°. (Design tolerances for this component are usually limited to $\pm 1°$ [11], [14].) It is believed that this discrepancy is caused by relative convergence phenomena of the generalized TE–TM mode analysis (method 3). Particularly in the case of a TE_{10} mode excitation, this method matches also the (vanishing) E_x field component in the discontinuity plane [16] and, consequently, requires a considerably larger number of modes than the TE^x_{mn} procedure where the $E_x = 0$ condition is directly incorporated. Therefore, the results of Fig. 7(a) also imply a convergence improvement in favor of the TE^x_{mn} procedure compared with the generalized TE–TM mode analysis. The calculation of the VSWR behavior (Fig. 7(b)) is relatively insensitive to the number of modes. The results of an eight and a 35 mode analysis are within the plotting accuracy and agree closely with the data presented in [16].

IV. Conclusions

A modified TE^x_{mn} mode approach for waveguide double-plane discontinuity modeling is presented and compared with alternative mode matching techniques. The applicability of the new approach matching E_y and H_x or H_y field components alternatively is demonstrated, whereas mode matching utilizing only E_y and H_x field components turned out to be unsuitable for general applications. With storage savings of more than 50% and CPU time reductions down to 20% with maintained accuracy and improved phase convergence compared with the generalized TE–TM procedure, the new TE^x_{mn} mode method offers an attractive solution for the numerically efficient yet accurate computer-aided design of waveguide components involving double-step discontinuities.

References

[1] G. Matthaei, L. Young, and E. M. T. Jones, *Microwave Filters, Impedance-Matching Networks, and Coupling Structures.* Dedham, MA: Artech House, 1980.

[2] T.-S. Chen, "Characteristics of waveguide resonant-iris filters," *IEEE Trans. Microwave Theory Tech.*, vol. MTT-15, pp. 260–262, Apr. 1967.

[3] H. Patzelt and F. Arndt, "Double-plane steps in rectangular waveguides and their application for transformers, irises, and filters," *IEEE Trans. Microwave Theory Tech.*, vol. MTT-30, pp. 771–776, May 1982.

[4] F. Arndt, U. Tucholke, and T. Wriedt, "Computer-optimized multisection transformers between rectangular waveguides of adjacent frequency bands," *IEEE Trans. Microwave Theory Tech.*, vol. MTT-32, pp. 1479–1484, Nov. 1984.

[5] U. Tucholke, "Feldtheoretische Analyse und rechnergestützter Entwurf von Resonanzblendenfiltern und Rillenpolarisatoren in Rechteckhohlleitern," VDI-Verlag, Düsseldorf, West Germany, 1988.

[6] W. Hauth, R. Keller, and U. Rosenberg, "CAD of waveguide low-pass filters for satellite applications," in *Proc. 17th European Microwave Conf.*, Sept. 1987, pp. 151–156.

[7] G. E. Craven and C. K. Mok, "The design of evanescent mode waveguide bandpass filters for a prescribed insertion loss characteristic," *IEEE Trans. Microwave Theory Tech.*, vol. MTT-19, pp. 295–308, Mar. 1971.

[8] Y. C. Shih and K. G. Gray, "Analysis of evanescent-mode waveguide dielectric resonator filters," in *IEEE MTT-S Int. Microwave Symp. Dig.*, June 1984, pp. 238–239.

[9] Q. Zhang and T. Itoh, "Computer-aided design of evanescent-mode waveguide filter with nontouching *E*-plane fins," *IEEE Trans. Microwave Theory Tech.*, vol. 36, pp. 404–412, Feb. 1988.

[10] J. Bornemann and F. Arndt, "Rigorous design of evanescent-mode *E*-plane finned waveguide bandpass filters," in *IEEE MTT-S Int. Microwave Symp. Dig.*, June 1989, pp. 603–606.

[11] R. J. Dewey, "Circularly polarized elliptical beamshape horn antennas," *Int. J. Electron.*, vol. 53, no. 2, pp. 101–128, 1982.

[12] E. Kühn and B. K. Watson, "Rectangular corrugated horns—Analysis, design and evaluation," in *Proc. 14th European Microwave Conf.*, Sept. 1984, pp. 221–227.

[13] A. J. Simmons, "Phase shift by periodic loading of waveguide and its application to broad-band circular polarization," *IRE Trans. Microwave Theory Tech.*, vol. MTT-3, pp. 18–21, Dec. 1955.

[14] G. A. E. Crone, N. Adatia, B. K. Watson, and N. Dang, "Corrugated waveguide polarizers for high performance feed systems," in *IEEE AP-S Int. Symp. Dig.*, 1980, pp. 224–227.

[15] F. Arndt, U. Tucholke, and T. Wriedt, "Broadband dual-depth *E*-plane corrugated square waveguide polariser," *Electron. Lett.*, vol. 20, pp. 458–459, May 1984.

[16] U. Tucholke, F. Arndt, and T. Wriedt, "Field theory design of square waveguide iris polarizers," *IEEE Trans. Microwave Theory Tech.*, vol. MTT-34, pp. 156–160, Jan. 1986.

[17] T. Itoh, *Numerical Techniques for Microwave and Millimeter-Wave Passive Structures.* New York: Wiley, 1989, ch. 9.

[18] R. Vahldieck and B. Varailhon de la Filolie, "Computer-aided design of parallel-connected millimeter-wave diplexers/multiplexers," in *IEEE MTT-S Int. Microwave Symp. Dig.*, May 1988, pp. 435–438.

[19] R. Vahldieck and B. Varailhon de la Filolie, "A novel waveguide quadruplexer for millimeter wave applications," in *Proc. 19th European Microwave Conf.*, Sept. 1989, pp. 621–626.

[20] J. Bornemann and F. Arndt, "Modal-*S*-matrix design of optimum stepped ridged and finned waveguide transformers," *IEEE Trans. Microwave Theory Tech.*, vol. MTT-35, pp. 561–567, June 1987.

[21] R. Vahldieck and W. J. R. Hoefer, "Finline and metal insert filters with improved passband separation and increased stopband attenuation," *IEEE Trans. Microwave Theory Tech.*, vol. MTT-33, pp. 1333–1339, Dec. 1985.

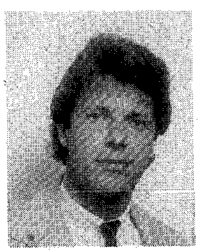

Jens Bornemann (M'87–SM'90) was born in Hamburg, West Germany, on May 26, 1952. He received the Dipl.-Ing. and Dr.-Ing. degrees, both in electrical engineering, from the University of Bremen, West Germany, in 1980 and 1984, respectively.

From 1980 to 1983, he was a Research and Teaching Assistant in the Microwave Department at the University of Bremen, working on quasi-planar waveguide configurations and computer-aided *E*-plane filter design. After a two-year period as a consulting engineer, he joined the University of Bremen again, in 1985, and was employed at the level of Assistant Professor. Since April 1988, he has been an Associate Professor at the University of Victoria, Victoria, B.C., Canada. His current research activities include microwave system design, active components, and problems of electromagnetic field theory.

Dr. Bornemann was one of the recipients of the A.F. Bulgin Premium of the Institution of Electronic and Radio Engineers in 1983. He serves on the editorial board of the IEEE TRANSACTIONS ON MICROWAVE THEORY AND TECHNIQUES and has authored or coauthored more than 40 technical papers.

Ruediger Vahldieck (M'85–SM'86) received the Dipl.-Ing and Dr.-Ing. degrees in electrical engineering from the University of Bremen, Bremen, West Germany, in 1980 and 1983, respectively.

From May 1984 to June 1986 he was a Research Associate at the University of Ottawa, Ottawa, Canada, and in July 1986 he joined the Department of Electrical and Computer Engineering at the University of Victoria, Victoria, B.C., Canada, where he is now an Associate Professor. His research interests include numerical methods to solve electromagnetic field problems for the computer-aided design of microwave and millimeter-wave integrated circuits, FET amplifiers, couplers, and nonreciprocal devices. The emphasis of his work is on quasi-planar filters and filters for MMIC application.

Dr. Vahldieck, together with three coauthors, received the outstanding publication award of the Institution of Electronic and Radio Engineers in 1983. He is on the editorial board of the IEEE TRANSACTIONS ON MICROWAVE THEORY AND TECHNIQUES and has published 40 technical papers in the field of microwave CAD. He teaches professional short courses at George Washington University, Washington, DC, on numerical techniques in electromagnetics.